Rad-hard, Ultra-fast, InGaAs Photodiodes for Space Applications

Abhay M Joshi*, Frank Heine**, and Thomas Feifel**
*Discovery Semiconductors, Inc. 119 Silvia St, Ewing, NJ 08628, USA
**Tesat Spacecom GmbH, Co.KG, Gerberstr. 49, 71522, Backnang, Germany

ABSTRACT

We have manufactured rad-hard, InGaAs photodiodes using our proprietary Dual-Depletion Region (DDR) technology with bandwidths exceeding 10 GHz. The devices demonstrate high reliability and superior RF performance, thus, making them ideal for deployment in space for applications such as LIDAR and optical intersatellite links. The responsivity at 1064 nm is >0.45 A/W with optical return loss of 40 dB. The photodiodes have broad wavelength coverage from 800 nm to 1700 nm, and thus can be used at several wavelengths such as 850 nm, 1064 nm, 1310 nm, 1550 nm, and 1620 nm. The InGaAs photodiodes exhibit very low Polarization Dependence Loss (PDL) of 0.05 dB typical to 0.1 dB maximum. The typical Failure-in-time (FIT) values of these photodiodes are 0.011 and 15.384 at 25ºC and 75ºC respectively. FIT is defined as the number of failures per billion hours of operation. The photodiodes have been tested for different radiation tests such as 50 kRad gamma (Co 60) and protons with a fluence of 3 x 10^{11} p/cm^2, and have passed typical qualification levels of random vibration.

Keywords: InGaAs photodiodes, ultra-fast, rad-hard, gamma radiation, proton radiation, vibration, responsivity, and dark current.

1. INTRODUCTION

Since 1995, Discovery Semiconductors (DSC) has pioneered a high-speed photodetector technology known as the "**dual-depletion**" p-i-n photodetector [1]. This design allows good responsivity, high speed, and high saturation currents from a front-illuminated photodiode that is relatively easy to manufacture and integrate. Figure 1 shows the schematic of dual depletion layer InGaAs/InP photodetector.

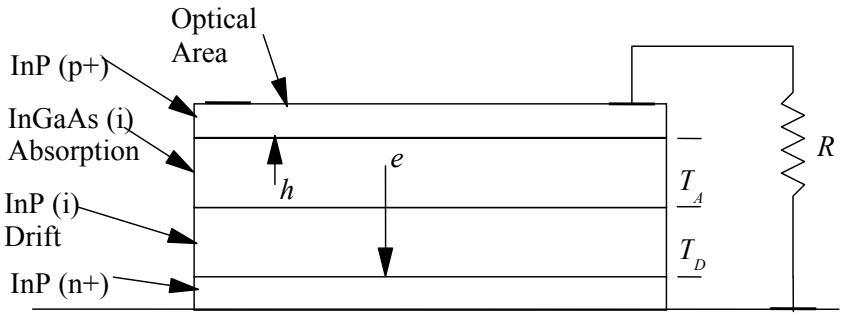

Figure 1. Schematic of Discovery Semiconductors' high speed, high power handling, dual-depletion layer InGaAs/InP heterostructure p-i-n photodetector. The optical area was 30 or 40 μm diameter for this space program giving a bandwidth of 10 GHz and higher.

InGaAs photodiodes made by DSC are suitable for multiple applications and environments. Fiber pigtailed photodiode modules are used as part of the fiber-optics infrastructure backbone, both for terrestrial and submarine networks, as well as in space applications. DSC is providing the 10 GHz InGaAs photodiode for the Aladin Reference Laser Head (RLH). The Flight Models of that Laser are currently being assembled at Tesat Spacecom of Germany and described in section 5. The RLH acts as a seed laser for the ALADIN UV LIDAR. This LIDAR will measure the global wind field

*Abhay@chipsat.com; phone 1 609 434 1311; fax 1 609 434 1317; www.chipsat.com

Spaceborne Sensors III, edited by Richard T. Howard, Robert D. Richards,
Proc. of SPIE Vol. 6220, 622003, (2006) · 0277-786X/06/$15 · doi: 10.1117/12.666055

during the ESA AEOLUS mission. The 10 GHz, DSC30 photodiode module has passed several tests like gamma radiation, proton radiation, and launch vibrations to determine if it can survive the harsh environments of launch and space operations. The details will be discussed further in this paper. The wavelength response plot for the dual-depletion InGaAs photodiode is shown below in Figure 2. As can been seen from the figure below, the photodiodes have broad wavelength coverage from 800 nm to 1700 nm, and thus can be used at several wavelengths such as 850 nm, 1064 nm, 1310 nm, 1550 nm, and 1620 nm.

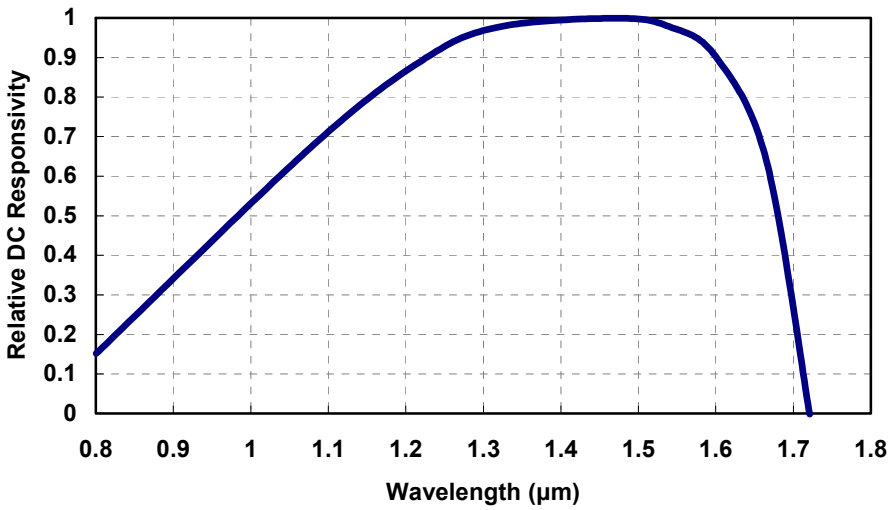

Figure 2. Wavelength response of InGaAs/InP photodiode. For Aladin system, the photodiode is used at 1064 nm.

2. RAD-HARD, ULTRA-FAST, InGaAs PHOTODIODES

Several researchers have studied the radiation effects on InGaAs PIN photodiodes [2, 3]. The severe increase in the dark current, especially the generation-recombination (g-r) current due to radiation damage has been a major concern and may be attributed to the lattice damage (displacement damage) caused by radiation to the low band gap InGaAs epitaxial layer [2, 3]. This prior study had InGaAs photodiodes whose InGaAs absorption region was thick, about 3 to 4 microns [4]. Such thick absorber may be a problem in designing and manufacturing rad-hard InGaAs photodiodes. To keep the radiation damage minimal, we designed the photodiodes whose InGaAs absorber is only 1.25 microns in thickness. Thus, an ultra-fast, dual-depletion InGaAs/InP photodiode with a thinner InGaAs absorber may be inherently more rad-hard as compared to the prior InGaAs photodiodes. The data in the section 3 proves the rad-hard nature of these photodiodes.

The basic band structure for an unbiased dual-depletion, InGaAs/InP heterojunction photodiode is shown in Figure 3. One can see that an energy well exists for the electrons but not for the holes. When a bias voltage is applied, the band diagram is modified in two ways, as shown in Figure 4. First, thin layers of the p+ and n+ doped regions are depleted. This induces an electric field in the undoped region. Second, the Fermi energy, indicated by the dashed line (and all the other energies) has a negative slope in presence of the electric field.

In desired operation, the electrons will flow down the energy gradient from the InGaAs region to the n+ doped InP region. The holes will flow up the energy gradient from the InGaAs region into the p+ InP region. In the present structure, however, the barrier in region 1 will impede the electron motion, and the barrier in region 2 will impede the holes. To maintain good current handling capacity as well as linearity, the recommended reverse bias is +3V to +7V. This produces sufficient electric field for the charge carriers, both holes and electrons, to overcome these barriers.

The basic issues for high bandwidth detectors are the electrical capacitance of the detector and the transit time for carriers in the detector. For high optical input power, we must also consider the non-linear effects of space-charge effects, barrier trapping, and saturation. In the design process, one must balance all of these factors to achieve the

optimum detector performance. This balance can be found by analyzing the underlying physics of carrier motion through a p-i-n structure.

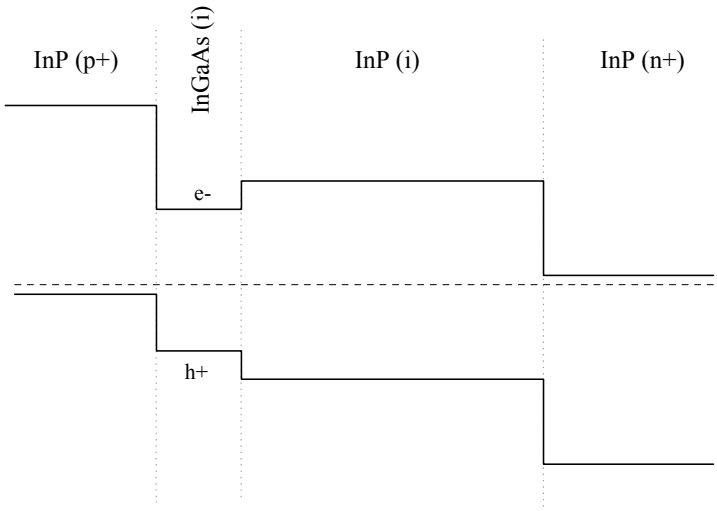

Figure 3. The basic InGaAs/InP heterojunction dual-depletion photodiode at zero bias.

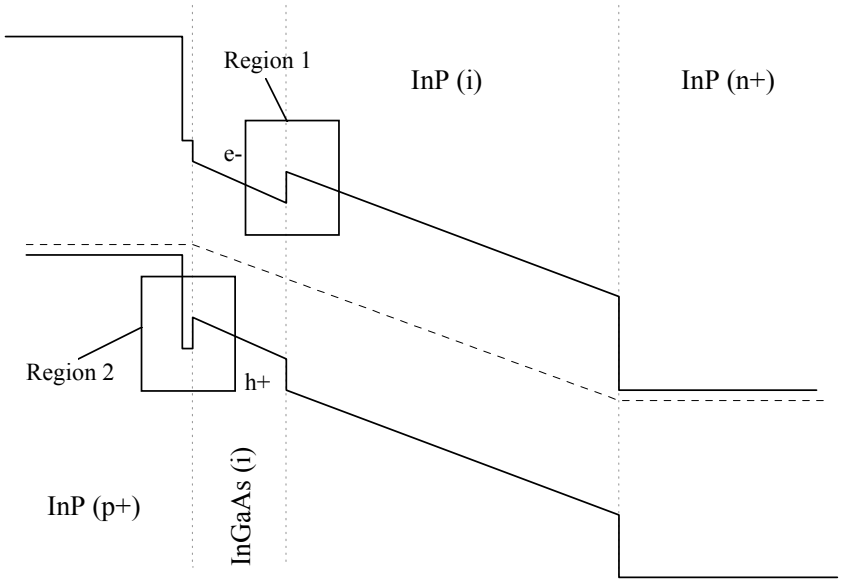

Figure 4. The basic dual-depletion diode under strong reverse bias voltage. Both the electrons and the holes have a barrier to overcome in order to reach the p+ and n+ electrodes.

When the semiconductor is operating in the linear regime, the two major limits on device speed are the capacitive time-constant and the carrier transit-time. As analyzed in our previous work [5], there are two major capacitances to consider in optical detectors: the intrinsic capacitance of the diode itself, and the parasitic capacitance of the preamplifier circuitry. The intrinsic capacitance, $C_{Int.}$, is given by the simple parallel plate capacitance of the p-i-n structure, and is proportional to the area and permittivity, A and ε, and to the inverse of the depletion region thickness, d.

$$C_{Int} = \frac{\varepsilon A}{d}. \quad (1)$$

This capacitance, in association with the load resistance of the amplifier, R, determines the electrical time constant of detection, τ_{RC}.

$$\tau_{RC} = RC_{Int.}. \quad (2)$$

Hence, the capacitance needs to be minimized and requires the depletion region (d) to be thick. The transit time, τ_{TR}, is the time required for the photogenerated carriers in the i region of the detector to move to the electrode surfaces. Given that the carriers are moving at their saturation velocities, v, the transit time is proportional to the intrinsic thickness, as given by Eq. (3),

$$\tau_{TR} = \frac{d}{v}. \quad (3)$$

This time gives the limit of the duration of the impulse response of the detector. Thus, a thick detector will have a long transit time, and thus a slow response.

Fortunately, the properties of InGaAs and InP are such that the electrons can travel as much as ten times faster than the holes at certain electric fields [5]. By fabricating the detector such that the carriers are generated only near the p contact, as shown in Figure 5, a large speed increase can be realized. When the carriers are generated near the p contact, the slower holes travel a shorter distance than the faster electrons. This allows a thicker intrinsic region without the transit time penalty.

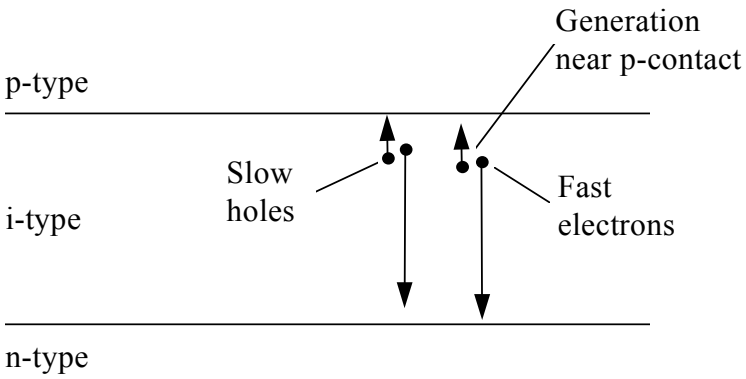

Figure 5. A generic p-i-n detector structure, illustrating how selective carrier generation can accelerate the transit time effect because of the difference in hole and electron velocities.

Our previous work involved making detectors as small as 10 μm in diameter with response speeds up to 65 GHz [6]. The selective carrier generation was accomplished by fabricating an InGaAs / InP dual-depletion detector as shown in Figure 1. This works by using two different compositions of semiconductor in the depletion region: one absorbing (InGaAs) and one transparent (InP). The carriers are generated only in the absorbing material, and by placing the absorbing material adjacent to the p contact, the transit time is improved. Using the carrier drift models developed previously [1, 6], we can re-optimize the design of the detector to achieve a 100 GHz response [7].

The SEM photograph of the DSC30 InGaAs photodiode used in the Aladin system is shown in Figure 6. The detail processing and fabrication of these photodiodes is explained else where [1, 6]. As shown in Figure 6, the photodiode has a GND-SIG-GND co-planar electrical output which allows for easy assembly and integration with the following

electronics, for e.g., a Transimpedance Amplifier (TIA). Figure 7 shows the frequency response plots of two DSC30 photodiodes A and B which were used for proton radiation exposure as explained in the section 3. Additionally, Diode C (DSC40S) was used for gamma radiation effects. Table I lists the key measured parameters for Diodes A, B, and C at 22ºC prior to the radiation exposure. Diodes A and B were our product type DSC30 and Diode C was DSC40S. The DSC30 has no 50Ω internal termination resistor, whereas DSC40S has an internal 50Ω termination resistor [8].

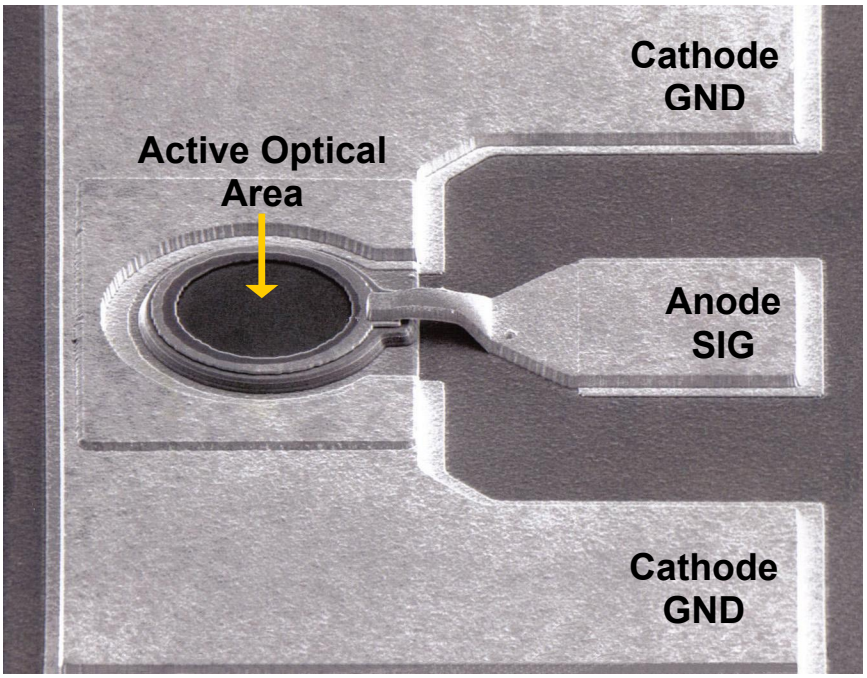

Figure 6. The SEM photograph of the DSC30 top illuminated, InGaAs photodiode used in the Aladin system. The photodiode is mounted on an Alumina substrate along with supporting passive components. The diameter of the photodiode is 30 microns.

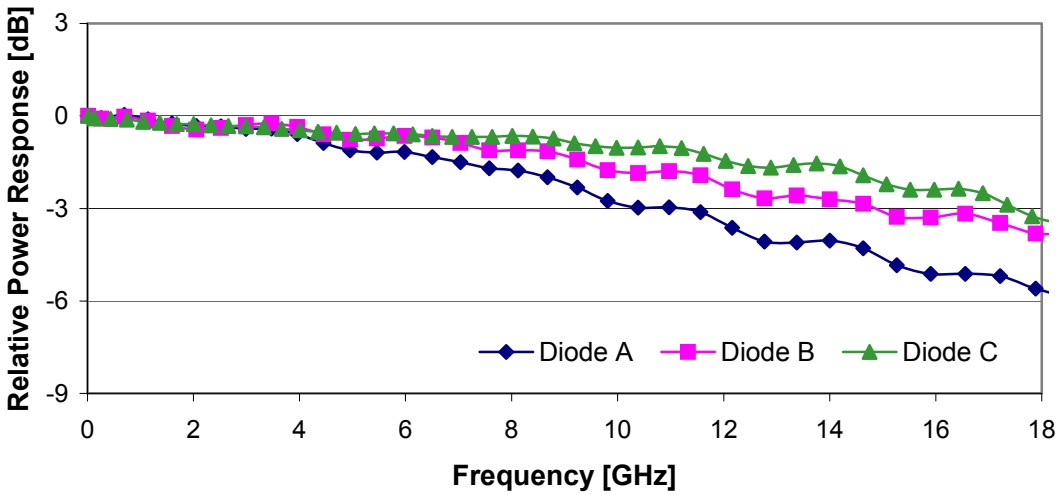

Figure 7. Frequency response of two DSC30 photodiodes, A and B, used for proton radiation testing. Diode C which is a DSC40S was gamma radiated and has a diameter of 40 microns.

Table I: Pre-radiation Device Characteristics

Parameter	Diode A	Diode B	Diode C
-3dB Bandwidth (GHz)	11.2	15	17.5
Responsivity at 1310 nm (A/W)	0.98	0.78	0.82
Dark current at V_{bias} +5V, 22ºC (nA)	5	6	10

The following section will evaluate any changes in the above characteristics with proton and gamma radiation.

3. RADIATION TESTING of ULTRA-FAST, InGaAs PHOTODIODES

In the space environment, semiconductor devices such as lasers, transistors, opto-couplers, photodiodes, and LEDs are prone to malfunctioning due to the exposure to high energy particles such as protons, neutrons, electrons or photons such as gamma rays and X-rays [9, 10]. It is very difficult to shield high energy protons as their penetration depth is too large. Even gamma rays are known to penetrate quite easily through an Aluminium shield [11]. Thick barriers like concrete, lead, or water are used on Earth to block high energy protons or gamma rays. Unfortunately, these techniques are not practical on a spacecraft as it increases its weight. With launch costs approaching US$10,000 to 12,000 per pound of spacecraft, there is a limitation to using thick barriers against high energy particles. Thus, it is mandatory that key electronic components like the ultra-fast, InGaAs photodiode be tested for radiation effects.

3.1. Proton Radiation Experimental Results

The Fraunhofer Institut für Naturwissenschaftlich-Technische Trendanalysen (INT) carried out a 35 MeV proton irradiation of InGaAs photodiode modules (PD) type DSC30 during September 2005 for TESAT Spacecom GmbH (Tesat). The devices under test (DUT) were irradiated at the proton irradiation facility of the INT at the injector cyclotron JULIC of the Forschungszentrum Jülich (FZJ, Research Centre Julich).

The energy of the beam is fixed to 45 MeV in vacuum, with a maximum current of 10 μA (i.e. 6 x 10^{13} s^{-1}). During the irradiation the beam current was set as low as possible (10 nA) because of the low requested fluences in the order of a few times 10^{11} cm^{-2} [12]. The particles are concentrated in a small focus of less than 1 cm diameter inside the beam pipe. For simplicity, the irradiations take place outside the beam pipe in air. So the protons have to pass a 2 mm thick Aluminium (Al) sheet which reduces the available energy to 39 MeV [12]. The effective energy is further reduced to about 35 MeV because the protons have to cross 2.5 m of air before reaching the target station. Due to the scattering inside the Al exit window and with the air molecules, the usable beam diameter at the target area is about 20 cm.

With the help of a position-sensitive ionisation chamber (PSIC), the beam is shifted horizontally and/or vertically until it is concentrically around our target station before irradiation of the DUT. So all DUT will be irradiated with the same fluence afterwards. The DUT are plugged into sockets mounted on a printed circuit board (PCB) directly in front of the location of the PSIC. Also copper foils are put onto the PCB to measure the proton fluence by activation analysis. This is shown in Figure 8 [12].

The 35 MeV proton fluxes were 3.1 and 3.5 × 10^{8} $cm^{-2}s^{-1}$ for the two photodiodes, A and B during the three irradiation steps. The slight difference in the proton flux results from alignment problems of the beam axis during irradiation which could not be solved by simply steering the beam. The irradiation times were 300 s for each step. The time interval between the completion of an exposure to the start of the next exposure was less than 20 minutes. Device A was exposed up to a fluence of 2.8 × 10^{11} cm^{-2} during three subsequent exposures with fluences of 3.1 × 10^{8} cm^{-2} whereas device B reached a total fluence of 3.2 × 10^{11} cm^{-2} with fluences of 3.5 × 10^{8} cm^{-2} for each step. The uncertainties of the fluence values are 13%.

The corresponding equivalent doses in InGaAs are 51 and 59 kRad(InGaAs). The equivalent dose rates of 57 and 65 Rad(InGaAs)/s are above the requested value of 20 rad/s because of the uncertainties in preparing the proton beam [12]. The error of the conversion is unknown and therefore not further mentioned. All the measured and derived values are summarized in Table II.

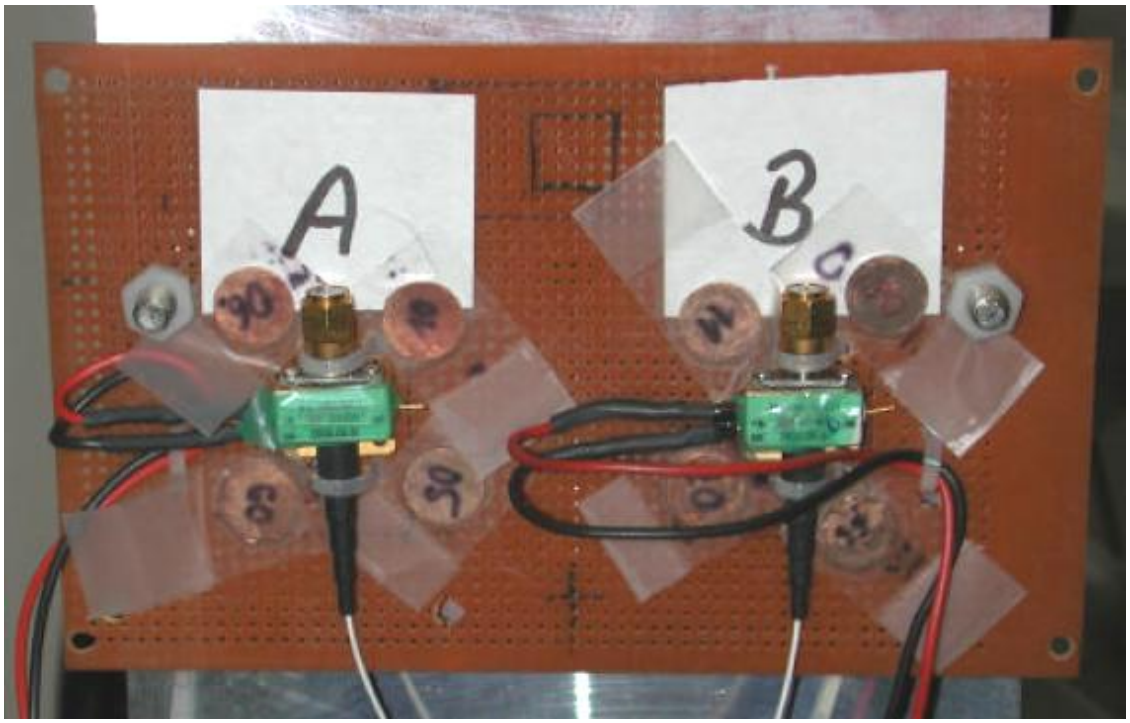

Figure 8. Set-up during the irradiation of the DSC30. Each DUT, labeled A and B, is surrounded by 4 copper activation analysis foils. The PDs are biased at + 2V during irradiation (black and red cables) and are connected via optical fibers (white cables) to 1300 and 1550 nm light sources [12].

Table II: Proton Fluence and Equivalent Dose Values During the Irradiation of the DSC30

DUT	A	B
Irradiation Time [s]	900	900
35 MeV Proton Flux [cm^{-2} s^{-1}]	$3.1 . 10^{8}$	$3.5 \cdot 10^{8}$
35 MeV Proton Fluence [cm^{-2}]	$2.8 \cdot 10^{11}$	$3.2 \cdot 10^{11}$
Error of Proton Fluence [%]	13	13
Equivalent Dose Rate [Rad(InGaAs)/s]	56.7	65.1
Total Equivalent Dose [kRad(InGaAs)]	51.0	58.6

3.1.1. Proton Radiation Exposure and Test Sequence

The sequence of steps for the radiation qualification are listed below:

a) Identification and marking of all components.
b) Initial room temperature electrical and optical characterization of all components.
c) Set-up of the proton cyclotron and bias of devices for irradiation.
d) Irradiation of the DUT up to a total fluence of about 1.0 x 10^{11} p/cm^2 with a flux of about 3 x 10^8 p/cm^2 s.
e) Room temperature electrical and optical characterization of all components.
f) Irradiation of the DUT up to a total fluence of about 2.0 x 10^{11} p/cm^2 with a flux of about 3 x 10^8 p/cm^2 s.
g) Room temperature electrical and optical characterization of all components.
h) Irradiation of the DUT up to a total fluence of about 3.0 x 10^{11} p/cm^2 with a flux of about 3 x 10^8 p/cm^2 s.
i) Room temperature electrical and optical characterization of all components.

3.1.2. Measurement Results

Table III shows the dark current (I_d) at +2V reverse bias, before and after the proton radiation. Figure 9 plots the data in Table III. As can been seen from Table III and Figure 9, there is a slight change in the dark current. Thus, the displacement damage due to protons is not significant in these ultra-fast, dual-depletion, heterostructure InGaAs/InP photodiodes. One thing to note though: room temperature may vary up to 5ºC which may lead to almost 65% variation in the dark current. Hence, the change in dark current is within the limits of the room temperature variation.

Table III: Room Temperature Dark Current at +2V Before and After High Energy Proton Irradiation of the DSC30

Photodiode A			
Fluence [10^{11}p/cm^2]	ΔFluence [10^{11}p/cm^2]	I_d [nA]	ΔI_d [nA]
0,00	0,00	3,56	0,12
0,93	0,12	4,35	0,14
1,85	0,24	4,43	0,14
2,78	0,36	4,60	0,15

Photodiode B			
Fluence [10^{11}p/cm^2]	ΔFluence [10^{11}p/cm^2]	I_d [nA]	ΔI_d [nA]
0,00	0,00	3,30	0,11
1,06	0,14	4,23	0,14
2,13	0,28	5,04	0,16
3,19	0,41	5,89	0,19

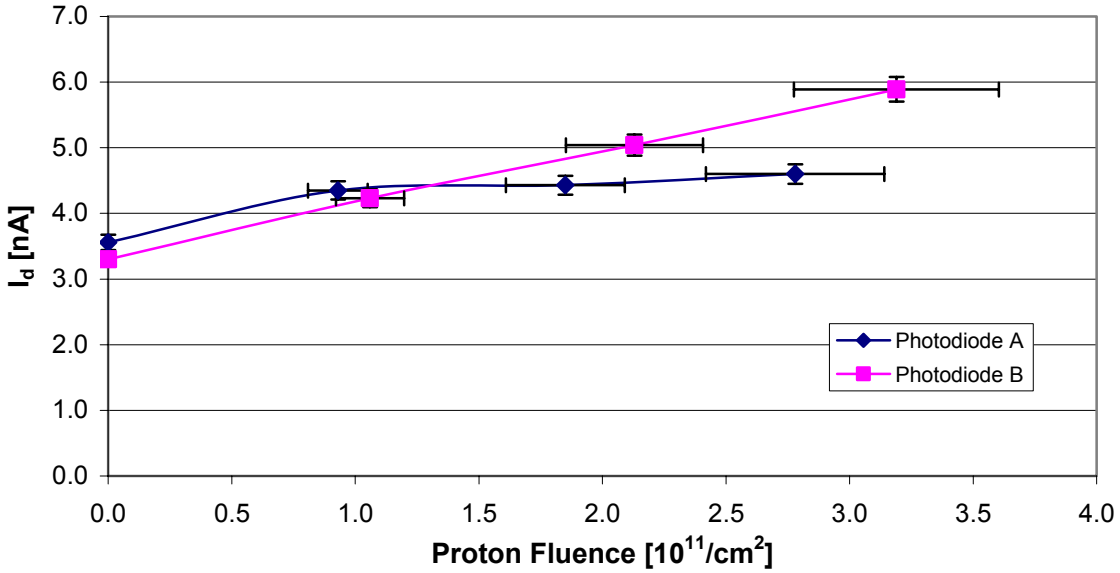

Figure 9. Room Temperature Dark Current before and after high energy proton irradiation of the DSC30, samples A and B shown in Table I. Reverse bias was +2V.

Figures 10 and 11 show the responsivity of the photodiodes A and B at 1550 nm and 1310 nm before and after the proton radiation. As seen from the figures, there was no change in the responsivity, thus, exhibiting rad-hard characteristics for the prescribed dose. These results also hold good at 1064 nm. The responsivity at 1064 nm is >0.45

A/W. DSC confirmed these results by checking the post-radiation characteristics of Diodes A & B for bandwidth, responsivity, and dark current. There was no change to the pre-radiation data as shown in Table I, thus indicating that proton radiation had no adverse effect on the photodiodes.

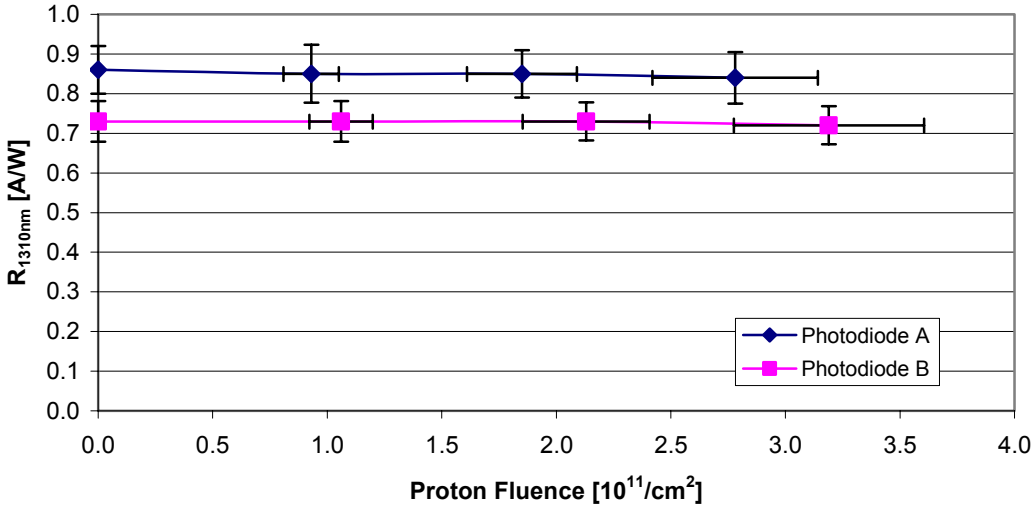

Figure 10. Responsivity at 1550 nm before and after high energy proton irradiation of the DSC30.

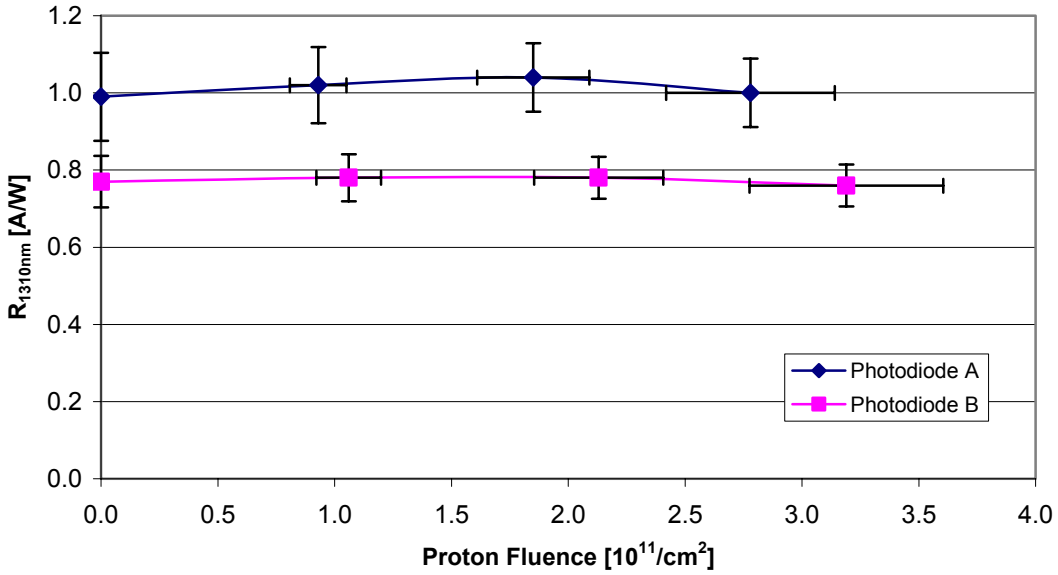

Figure 11. Responsivity at 1310 nm before and after high energy proton irradiation of the DSC30.

3.2. Gamma Radiation Experimental Results

The gamma radiation test was performed at the INT (Fraunhofer Institut für Naturwissenschaftlich Technische Trendanalysen) in Euskirchen (Germany). The probe setup was made in a way to guarantee a dose homogenity of 10% in a diameter of 125 mm. The vertical distance from the probes to the radioactive element (Co^{60}, energy is 1 MeV) was 200 mm, the fluence was 2.09 rad/s. in 399 min. The irradiation was carried out on between 2003-11-04 14:15 and 2003-11-04 20:54. The annealing time was set to 1 month, the post radiation test were started on 2003-12-04. The annealing was passive (without light / voltage applied to the DUTs) at ambient and in darkness.

The photodiode DSC40S was chosen for this test (Diode C in Table I & Figure 7 above). A severe degradation of the spectral or temporal response will degrade the performance of the Phase Locked Loop (PLL) at higher beat frequencies [13]. The measurements at Tesat are concentrated on the performance at 1064 nm (DC and AC response) in direct comparison with a diode from the same production lot (that is set as the reference). The results are summarized in Table IV.

Table IV: Post Gamma Radiation Results for Diode C

Property	**Change after 50 kRad gamma**
Photo diode DC response	No degradation was measurable
Photo diode AC response	No degradation was measurable

DSC confirmed Tesat's results in Table IV by checking post-radiation characteristics of Diode C for bandwidth, responsivity, and dark current. There was no change to the pre-radiation data as shown in Table I, thus indicating that gamma radiation had no adverse effect on the photodiode.

4. VIBRATION TEST RESULTS

The Discovery Semiconductors Photodiode (Type DC40S, Diode C in Table I and Figure 7) was successfully subjected to a random vibration test. The test was performed on 3 Axis with a load run of 2 minutes / each axis. The vibration level was 33 grams. No degradation in optical and electrical performance was measured as compared to the pre-vibration data shown in Table I. Figure 12 shows the Diode C on the shaker table, whereas Figure 13 shows the actual vibration load run. This successful test concluded the series of qualification tests for InGaAs photodiodes for the Aladin system.

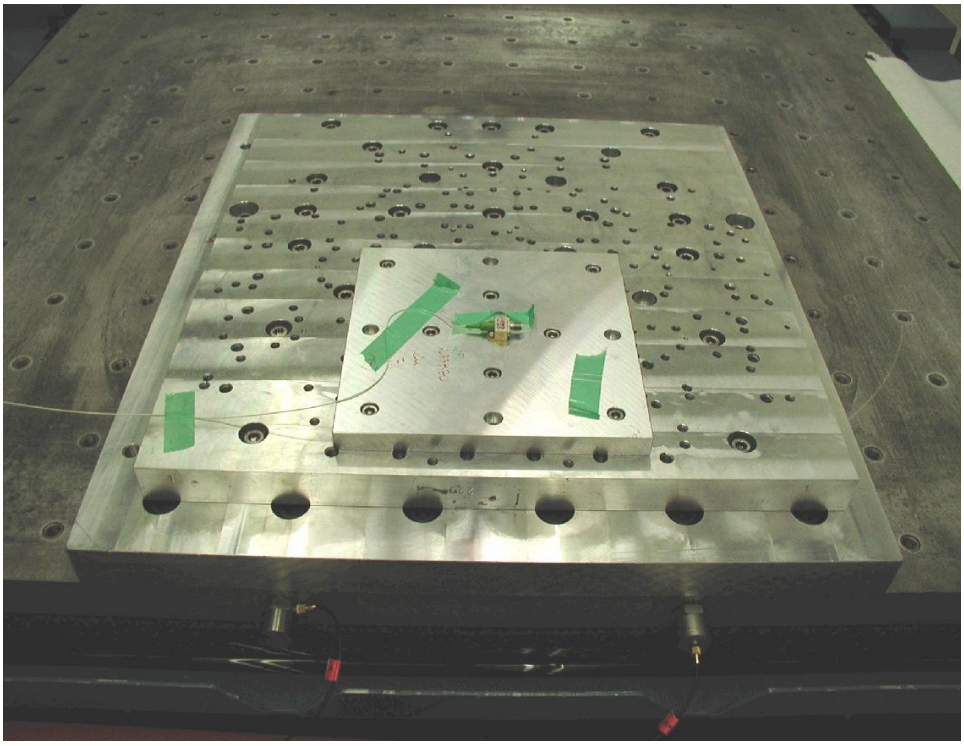

Figure 12. Discovery Semiconductors photodiode DSC40S (Sample C in Table I) on x-y shaker table.

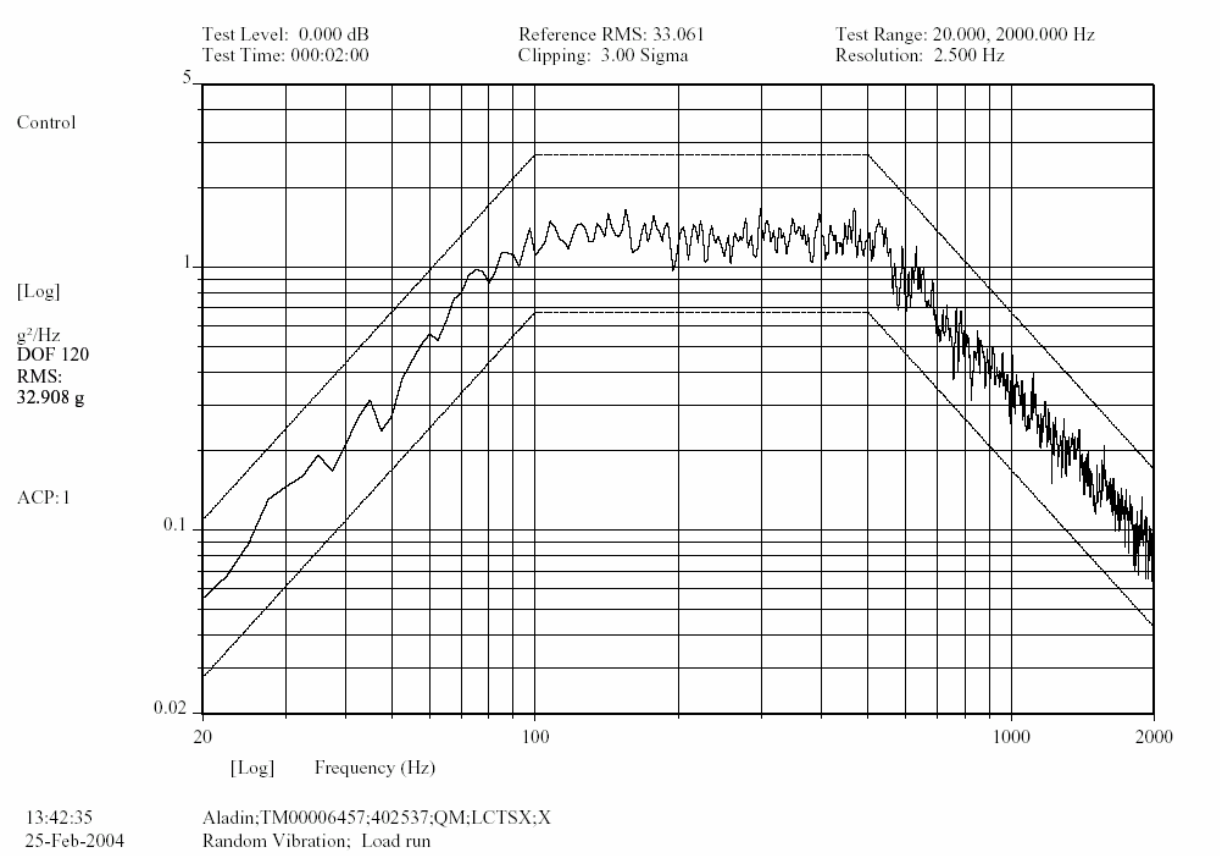

Figure 13. Effective load run spectrum: 1.3 g^2/Hz between 100Hz and 500 Hz.

5. SPACE APPLICATION of ULTRA-FAST InGaAs PHOTODIODE & ALADIN RLH

The previous sections illustrated that the Discovery's photodiodes DSC30 and DSC40S are qualified to exceed the various environmental and performance requirements of the ESA AEOLUS mission. Those include: (1) proton and gamma rays radiation hardness, (2) launch survivability, and (3) good electro/optical characteristics as listed in Table I.

In this section, the integration of the DSC photodiode into a TESAT laser is described. Some applications in space based LIDAR systems require high stability laser sources that can be precisely tuned to perform sensor calibration. The TESAT ALADIN Reference Laser Head (RLH) is such a laser and is shown in Figure 14. In order to simultaneously fulfill the stringent requirements of absolute frequency stability, low frequency drift, and fast step tuning performance of the AEOLUS mission, the approach for the RLH is to have separate tunability from frequency stabilization [13].

In the RLH, two TESAT single frequency lasers, Reference Laser (RL) and Seed Laser (SL) are built in as shown in Figure 15. One is locked to an optical reference cavity and is responsible for the frequency stability (approaching 2 x 10^{-11} ALLAN variance between 1 and 1000 sec). The light of the frequency stable laser is combined with the light of the seed laser (that is coupled to the down streams laser and amplifier chains) onto the 10 GHz photodiode (DSC30) and then locked and controlled via a digital PLL (Tesat development) as illustrated in Figure 15. This enables step tuning with a coarse (GHz / sec) rate and a fast fine tuning (8.3333MHz / 250 msec, 83.333 MHz / 950 msec). The step tuning performance is necessary for the LIDAR detector calibration and is shown in Figure 16 [13]. For more detailed explanation of the RLH, please review reference 13. The RLH acts as a seed laser for the ALADIN UV LIDAR. This LIDAR will measure the global wind field during the ESA AEOLUS mission.

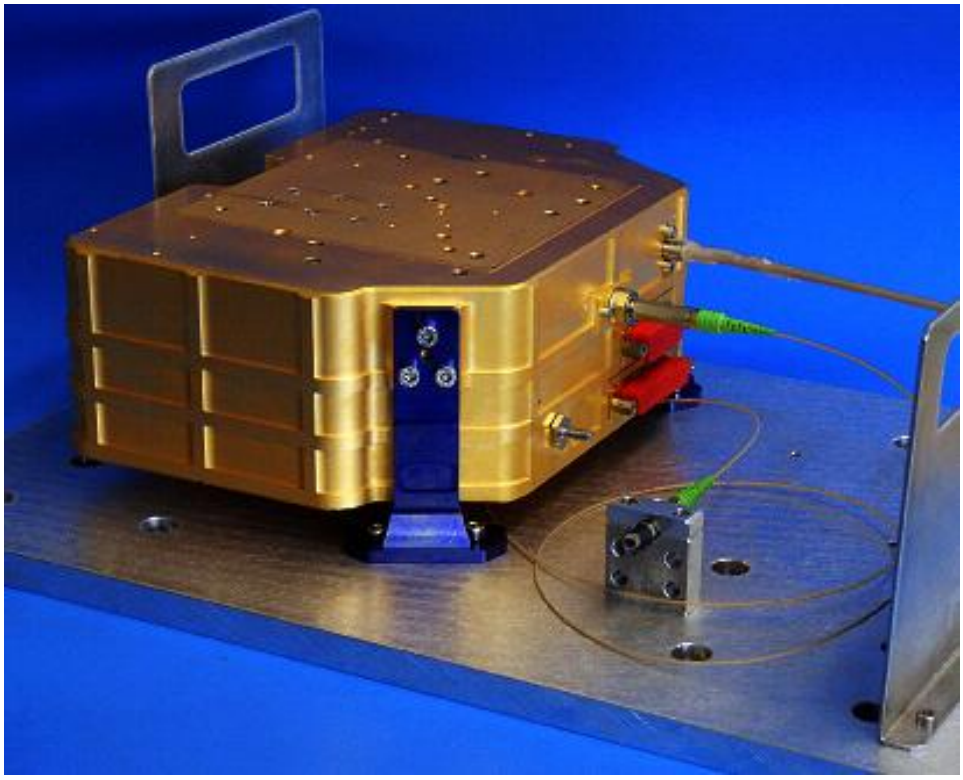

Figure 14. The ALADIN RLH (BB), isostatically mounted, thermal interface on top. Physical parameters: 2kg weight, 2 liter volume, 20W power consumption.

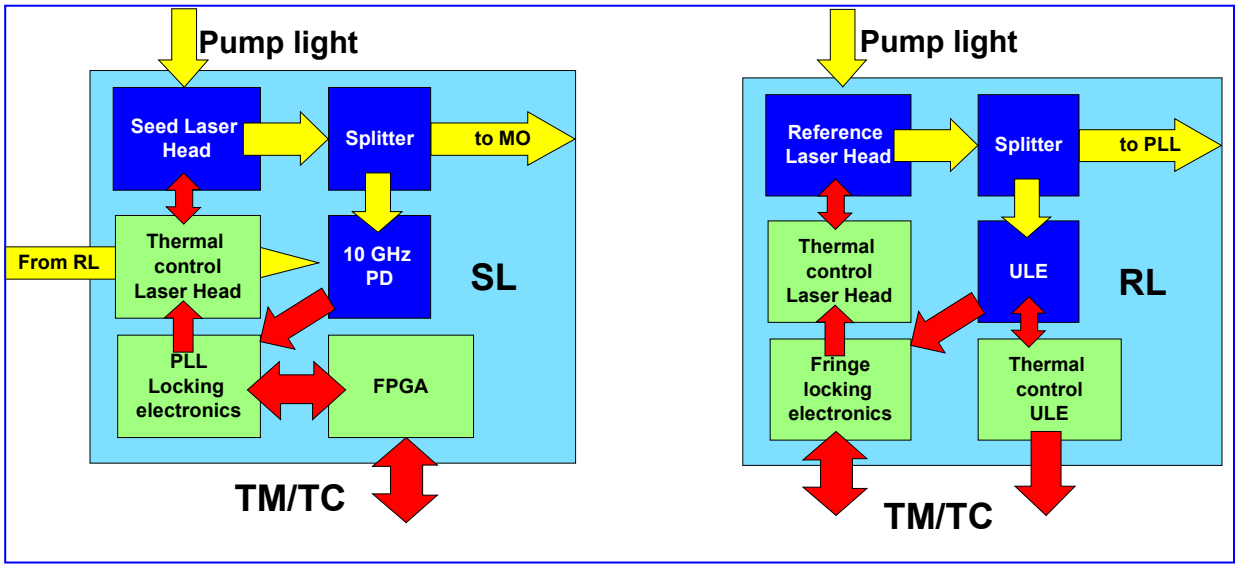

Figure 15. Functional architecture of the ALADIN RLH. SL is the seed laser, producing the tunable seed light for the ALADIN UV power laser. The frequency of the seed laser is controlled by combining a small fraction of the light with the light of the cavity stabilized reference laser (RL). The whole system is integrated into one box.

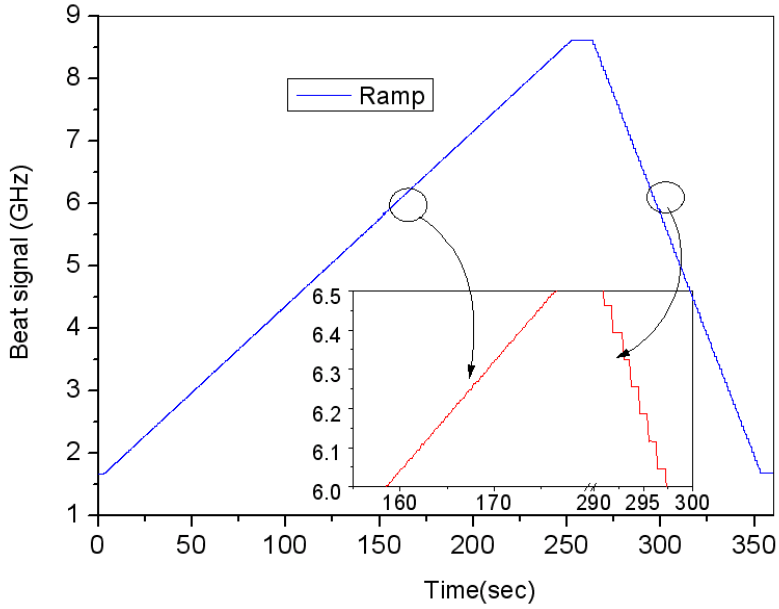

Figure 16. Measured step tuning performance, 1000 steps with 8.3333 MHz on the left, 100 steps with 83.333 MHz on the right.

6. CONCLUSIONS

In summary, Rad-hard InGaAs/InP photodiodes with bandwidths in excess of 10 GHz have been manufactured and qualified to exceed the various environmental and performance requirements of the ESA AEOLUS mission. Those include: (1) proton and gamma rays radiation hardness, (2) launch survivability, and (3) good electro/optical characteristics such as high responsivity & low dark current.

These rad-hard photodiodes are integrated into the TESAT ALADIN Reference Laser Head (RLH), thereby assuring that there is no degradation of the spectral or temporal response of the Phase Locked Loop (PLL) at higher beat frequencies [13].

7. ACKNOWLEDGMENT

The authors would like to thank their colleagues, Melissa Sweeney, Christoph Wree, and Don Becker for helping prepare this manuscript. We also thank Fraunhofer Institut für Naturwissenschaftlich Technische Trendanalysen (INT), especially Mr. Metzger and Mr. Lennartz, for the radiation testing of InGaAs photodiodes.

8. REFERENCES

1. A. M. Joshi and X. Wang, “DC to 50 GHz Wide Bandwidth InGaAs Photodiodes and Photoreceivers,” Proc. SPIE, Vol. CR73, pp. 181-196, 1999.
2. J. Troska, K. Gill, R. Grabit, and F. Vasey, “Neutron, proton, and gamma radiation effects in candidate InGaAs p-i-n photodiodes for the CMS tracker optical links,” CMS Note 1997/102, 1997.
3. R. J. Walters, G. J. Shaw, G. P. Summers, E. A. Burke, and S.R. Messenger, “Radiation Effects in $Ga_{0.47}In_{0.53}As$ Devices,” IEEE Trans. on Nuclear Sciences, Vol. 39. No. 6, pp. 2257-2264, 1992.
4. A. M. Joshi, G. H. Olsen, and S. R. Patil, “Reliability of InGaAs Detectors and Arrays,” Proc. SPIE, Vol. 1580, pp. 34-40, 1991.
5. F. J. Effenberger and A. M. Joshi, “Ultrafast, Dual-Depletion Region, InGaAs / InP p-i-n Detector,” J. of Lightwave Tech., Vol. 14, pp. 1859-1864, 1996.

6. A. M. Joshi, “DC to 65 GHz Wide Bandwidth InGaAs Photodiodes and Photoreceivers,” Mat. Res. Soc. Symp. Proc. Vol. 607, pp. 115-127, 2000.
7. D. A. Becker, A. M. Joshi, and D. R. Mohr, “100 GHz Dual-depletion InGaAs/InP Photodiode,” PSAA-10 DARPA Symposium, 2000.
8. Discovery Semiconductors, Inc. Data Sheet, “High Optical Power Handling Photodiodes to 20 GHz,” F720-14, Rev K, June 2005.
9. B. D. Evans, H. E. Hager, and B. W. Hughlock, “5.5 MeV Proton Irradiation of a Strained QW Laser Diode and a Multiple QW Broadband LED,” IEEE Trans. on Nuclear Sciences, Vol. 40, No. 6, pp. 1645-1654, 1993.
10. S. Humphrey, S. LaLumondiere, and S. Moss, “Lasers Simulate Space Radiation Effects,” The Aerospace Corp. Magazine of Advances in Aerospace Tech., Winter 2003.
11. “*Radiation and Life*”, E. J. Hall, Prof of Radiology, Columbia Univ, New York.
12. S. Metzger and W. Lennartz, Private Communications, “Proton Irradiation of Electronic Components, InGaAs Photodiode Module DSC30S,” Fraunhofer Institut für Naturwissenschaftlich Technische Trendanalysen (INT), October 2005.
13. F. Heine, K. Schieber, T. Meier, G. Mergenthaler, T. Schwander, R. Lange, and B. Smutny, “High Stability, Fast Tunable Single Frequency Laser Source for Space Based LIDAR Applications,” Proc. of 5th International Conf. on Space Optics, Vol. ESA SP-554, pp. 599-601, ICSO 2004.